Jurnal Polimesin
Department of Mechanical Engineering
Lhokseumawe State Polytechnic
http://e-jurnal.pnl.ac.id/polimesin
e-ISSN : 2549-1999 No : 2 Month : August
p-ISSN : 1693-5462 Volume : 20 Year : 2022

Article Info
Received : 2022-04-06 Accepted : 2022-07-21
Revised : 2022-07-21 Available online : 2022-08-31

Design and experimental test of runner blade for small axial pico-propeller turbines model

Pribadyo[1*], Hadiyanto[2], Jamari[3], Dailami[4]
[1]Department of Mechanical Engineering,
University of Teuku Umar, Meulaboh, 23615, Indonesia
[2]Department of Chemical Engineering,
University of Diponegoro, Semarang, 50275, Indonesia
[3]Department of Mechanical Engineering,
University of Diponegoro, Semarang, 50265, Indonesia
[4]Department of Mechanical Engineering, State Polytechnic of Lhokseumawe, Lhokseumawe, 24301, Indonesia
*Corresponding Author: pribadyo@utu.ac.id

Abstract

Environmental degradation due to the use of conventional fossil fuel remains an obstacle to sustainable development. For this reason, many countries currently consider the integration of renewable energy sources into their power sectors as an economically friendly and promising alternative to the use of fossil fuels. One form of green technology is the pico-propeller turbines. This turbine works based on the pressure of flowing water and its best performance is determined by the hydraulic stability of its blades. It is thus necessary to design suitable and hydraulically stable runner blades for these turbines. Therefore, this study aims to design a suitable runner blade for a pico-propeller turbine model that will aid in the optimal extraction of electrical energy from the fluid flow in sewer lines. The turbine wheel consists of four blades per section with a diameter of 0.150 meters and a pivot point of 0.30 meters and it was designed to fit a 5-inch diameter pipe with blade angle configurations of 25°, 30°, and 35°. Furthermore, performance tests were conducted at different flow rates, ranging from 0.00134 m3/s to 0.0047 m3/s with a 3.5 m head, after which the findings were compared to that of the other research. The results showed that maximum efficiency and performance were achieved with the blade angle of 25° at a flow rate of 0.0027 m3/s.

Keywords:
Small axial pico-propeller turbine, runner blades, design, experiment test

1 Introduction

The increasing use of conventional fuel energy technologies remains an obstacle to sustainable development. For this reason, the global community now considers the integration of renewable energy sources as a promising and economical prospect of green energy [1]. Furthermore, environmental factors play an important role in future power generation [2], and in the use of renewable energy sources including solar energy, biomass, geothermal, and hydropower, which has become a major focus in the world's energy sector. Several considerations led to promoting the use of hydropower as an energy source. These considerations include the fact that: hydropower is one of the renewable energy sources which has not been optimally utilized [3], hydropower is more efficient than wind and solar energy [4], it does not cause pollution, it is reliable, and it is cost-effective compared to the use of conventional fossil fuels as a source of energy [5, 6, 7]. Hydroelectric power is a green technology that can be generated by various types of turbines depending on the head and flow rate available at the location, as well as several other water-related conditions [8].

Currently, various types of water turbine technology have been developed both on a large and small scale, and the pico-propeller is a type of reaction turbine that generates power by combining water pressure and movement. It is usually used for low heads with relatively large discharges, and its runners comprise 2 to 6 blades and are placed directly in the river. The main aspect of pico-propeller turbines for small-scale power generation at low head conditions is that the turbine is capable of generating electricity with maximum output power leading to the Best Efficiency Point (BEP) [9]. In addition, the main component of these turbines is their runner blades, which directly convert the potential energy of the flow into mechanical energy through the rotation of the shaft. Therefore, it is necessary to pay special attention to the design of the turbine runner blades, as well as the turbine blade wedge. [10]. Furthermore, several studies have been conducted on turbine runner blades, both experimental and computational. [11, 12, 13]. The results showed that the shape of the blades can increase the turbine's efficiency by 73.9% [14], but an increased between-blade distance, flow coefficient, and head led to a decrease in shaft power and efficiency by 33 kW and 4%, respectively [15]. The previous study's runner blade design is shown in Fig 1.

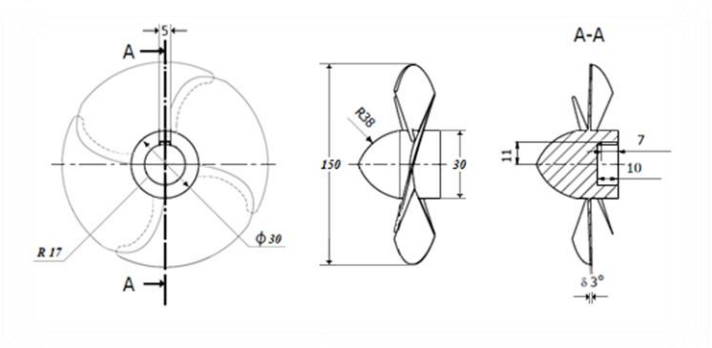

Fig 1. Runner Blade Design

Based on the results from previous studies, it is important to pay attention to not just the turbine's discharge, head, and specific speed parameters, but also to the parameters of its runner blades (such as the tilt angle, number of blades, and turbine diameter) when designing turbines for improved performance. Accordingly, the turbine blades in this study were designed to efficiently extract energy from the fluid flow in sewer lines. Three runner blade models were designed from the considered variations of the three angles of 25°, 30°, and 35°, after which they were tested in a pico-propeller turbine prototype which was developed for evaluation.

2 Methods

This study was conducted using several mathematical equations and experimental methods. Emphasis was laid on the purpose and concept of this experiment which includes the design planning, prototyping, testing, and measurement phases. The test and measurement data were then compiled into tables and graphs for further use in evaluating the turbine blade's performance.

Small-scale turbines (Pico) certainly cannot be designed such as large-scale turbines, and this is due to their difference in shape and size. Generally, small-scale turbines have low speed and this affects their ability to drive the generator at sufficient speed, which is why they cannot produce standard frequency power. Furthermore, reduction of the head is generally followed by a

decrease in flow velocity, and the speed of the moving objects, in this case, the generator also decreases. To achieve the same performance as a high-head turbine, the fluid's flow rate must be increased. The flow rate significantly impacts the turbine's diameter and rotation speed. A sketch of the head and a diagram of the process of converting water movement and pressure into electrical energy are shown in Fig 2.

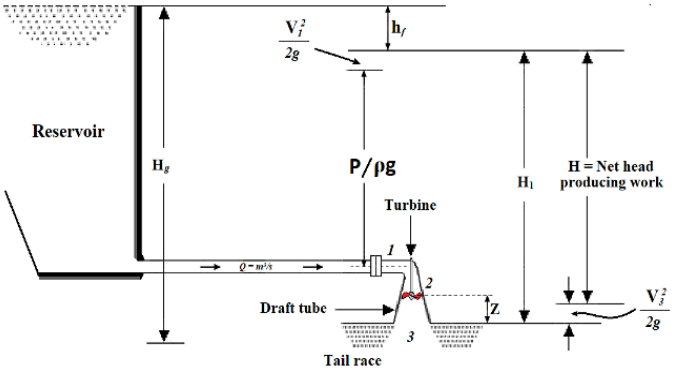

Fig 2. Head Sketch and Water Flow Process Diagram [16]

2.1 Design concept

A turbine's working capacity is generally dependent on its operating conditions and can be obtained by using the graph in Fig 3 [17]. Furthermore, turbines can be grouped according to their specific speeds, and their basic dimensions can be easily estimated once the specific speed is known. Various statistical studies in various schemes have been conducted to determine the specific speed correlation for each turbine type based on the net head. The specific speed was calculated using Equation (1) [16].

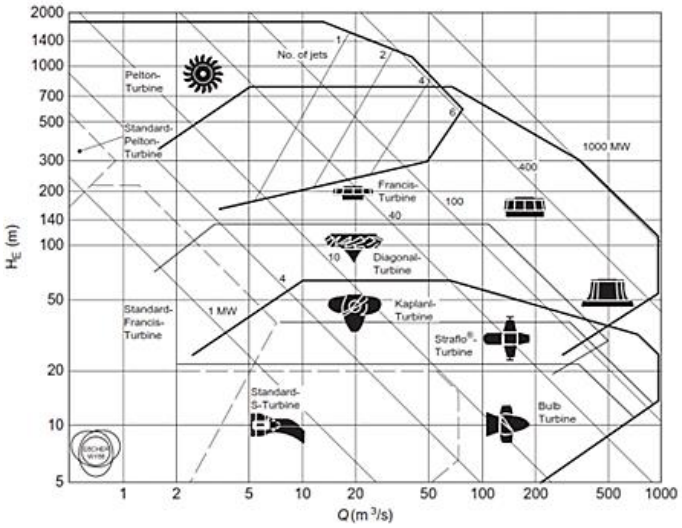

Fig 3. Turbine Selection Graph [18]

$$n_s = \frac{2.716}{H_n^{0.5}} \ (USBR) \tag{1}$$

Where H_n is the effective water drop height (m)

The propeller turbine of axial flow is a type of high-speed turbine because its blades move in the direction of the fluid flow, thereby making the blade's speed greater than the flow. The vectors acting on the turbine runner blades are shown in Fig 4.

To achieve the best efficiency and performance of a turbine, its blades must first be modified. The blade and hub make up a rotating part known as the turbine runner. Furthermore, achieving optimal performance by modifying the profile of the blade geometry should be carried out while taking into account the simplicity of its construction. Obviously, the design of a turbine runner blade is very complex. In this study however, the design was simplified.

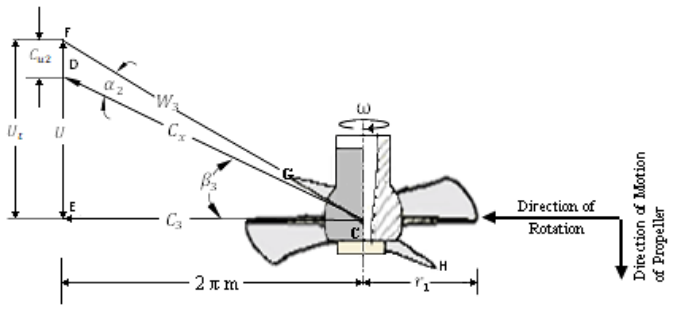

Fig 4. Vector Speed and Direction of Rotation of the Turbine Runner Blade [18, 19]

The turbine's capacity can be calculated using Equation (2).

$$P = \frac{\rho g Q H \eta_h}{1000} \tag{2}$$

Where Q is the flow of water (m^3/second), H is the height of the waterfall (m), η_h is the efficiency of the turbine (%), ρ is the density of water (kg/m^3), and g is the acceleration due to gravity (9.81 m/s^2).

2.2 Blade and hub design

The turbine blade and hub dimensions in each section were calculated using Equations (3) to (8).

$$D_e = 84{,}5 \times \left(0{,}79 + 1{,}602 \times n_{QE}\right) \times \frac{\sqrt{H_n}}{n} \tag{3}$$

$$D_i = \left(0{,}25 + \frac{0{,}0951}{n_{QE}}\right)^{*} D_e \tag{4}$$

$$A = (D_e^2 . D_1^2)\,\pi/4 \tag{5}$$

$$D_c = \frac{D_e + D_i}{2} \tag{6}$$

$$L = \frac{D_e - D_i}{2} \tag{7}$$

$$L_1 = \frac{D_c \times \pi}{z} \tag{8}$$

Usually, modifications are made to turbine design to determine the best blade alignment and optimize its efficiency [10]. The process of identifying the previously optimized model was carried out computationally by [20]. A schematic diagram of the flow direction and the runner blade's diameter with the velocity triangle on an axial flow turbine is shown in Fig 5.

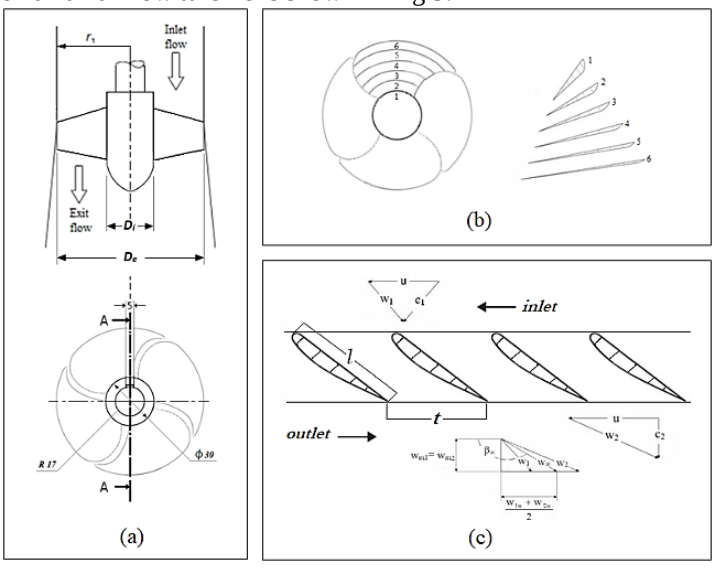

Fig 5. (a). A Schematic Diagram of Turbine Blades and Flow Direction at Input and Output, (b) Speed Triangle Grid, and (c) Cylindrical Cut on the Blade [18]

Tangential velocity (u) is the force exerted by the water that enters and exits the turbine. Its magnitude can be determined by Equation (9).

$$u = \pi * n \tag{9}$$

The absolute velocity (c) is the force released as soon as the flowing water hits the blade surface and can be determined by Equation (10).

$$c_{u1} = \frac{H_1 * g}{u} \tag{10}$$

The relative speed (w) is the force exerted by the turbine inlet and outlet and can be determined by Equations (11) to (14).

$$w_{u1} = c_{u1} = u \tag{11}$$

$$w_m = \frac{Q}{A_\infty} \tag{12}$$

$$A_\infty = \frac{\pi^*(D_e^2 - D_i^2)}{4} \tag{13}$$

$$w_\infty = \sqrt{w_{u\infty}^2 + w_m^u} \tag{14}$$

To obtain the accuracy of the angle of deviation, the angle of attack must be subtracted from the angle of glide (180-β∞) and this can be determined using Equation (15).

$$\beta_\infty = arccos \frac{W_{u\infty}}{w_\infty} \tag{15}$$

2.3 Turbine blade characteristics

This section discusses the steps taken to determine the main characteristics of the pico-propeller turbine blades.

1. Lift coefficient

The coefficient of lift for each radius can be determined by Equation (16).

$$\zeta_a = \frac{w_2^2 - w_\infty^2 + 2 \times g}{K^* W_\infty^2}$$

$$= \frac{\left[p_{atm} - H_s - p_{min} - \eta_s \times \frac{c_3^2 - c_4^2}{2^* g}\right]}{K^* W_\infty^2}$$

$$c_3 = \frac{Q}{A_3} \tag{16}$$

$$A_3 = \frac{\pi \times D_e^2}{4}$$

2. Rasio *l/t*

After the lift was known, the thickness of the turbine blades, which has the ratio l/t, was then determined using Equation (17).

$$t/l = \frac{1}{l/t} \Rightarrow \tag{17}$$

From Equation (12), the slip angle was assumed to be in the following range:

$$\lambda = 2{,}5° \div 3°$$

3. The reciprocal value of *l/t*

The reciprocal value of l/t was determined in advance. Through the reciprocal value, the ratio of the coefficient of lift obtained was ζ_a/ζ_A. Using this ratio, the coefficient of lift ζ_A was determined using Equation (18).

$$\frac{l}{t} = \frac{g \times \eta_{h \times H}}{w_\infty^2} \tag{18}$$

$$\times \frac{c_m}{u} \frac{\cos\lambda}{\sin(180 - \beta_\infty - \lambda)} \times \frac{1}{\zeta_a}$$

4. Drag force

information on the drag coefficient (ξ_w) of different profiles with each curve representing one of the profiles listed beside the graph as shows Fig 6. Furthermore, profile selection was carried out based on the complexity level of the shape and dimensions of the blade being planned.

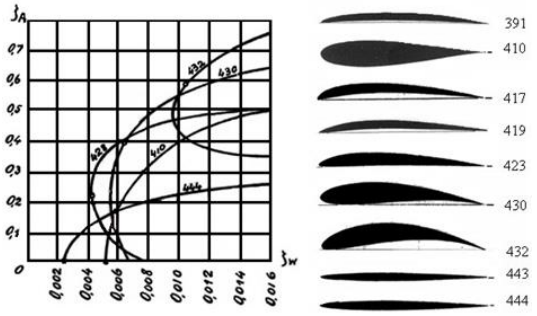

Fig 6. The Ratio of ζ_A and ζ_W for Different Profiles [21]

5. Slip angle

The slip angle was calculated to determine the turbine blade's inner diameter thickness using Equation (19).

$$\lambda = arctan \frac{\xi_w}{\xi_A} \tag{19}$$

6. Angle of attack

The angle of attack was calculated to determine the turbine blade's outer diameter and thickness, as shown in Fig 7 The angle of attack was calculated to determine the turbine blade's outer diameter and thickness, as shown in Fig 7.

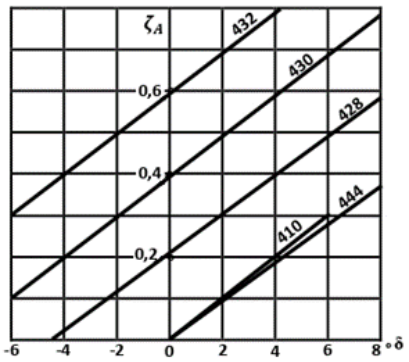

Fig 7. The Ratio of ζ_A and δ for Different Profiles [21]

2.4 Experimental testing method

The test experiment was designed by adjusting the pipe's shape and size to the location using direct measurements. The test location facilitated the measurement of flow rate and head used in the calculations. Furthermore, testing was conducted on each runner blade by adjusting the flow rate using valve openings 1 to 8 with detailed steps as follows:

1. Prepare the test equipment and measuring devices to be used.
2. Make sure the blade is correctly installed.
3. Set the blade for a 25° tilt angle on the turbine shaft and make sure it is installed properly.
4. Ensure there are no leaks.
5. Check the valve opening and make sure the available water flow is appropriate.

6. Ensure that the measuring tools are appropriate and can be used properly.
7. Do the test several times by adjusting the valve opening according to the planned discharge.
8. Measure the blade's number of rotations by placing a measuring instrument (digital tachometer) on the turbine shaft.
9. Record and document every process carried out.
10. Repeat steps 3 until 9 to test the turbine blades with a tilt angle of 30° and 35°.
11. After completing all the testing processes for the three turbine blade angles, clean the tool and test site.

To put it simply, the sequential test processes are shows Fig 8.

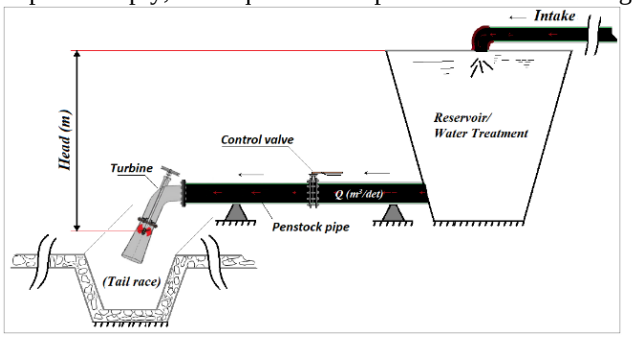

Fig 8. Schematic of the Test Layout

2.5 Research variable

1. Independent Variable

An independent variable is a variable that influences even the measured, manipulated, and selected factors of the study to determine the relationship between observed phenomena. The independent variables in this study are:

- The head was 3.5 meters.
- The flow rate variations, which were 0.00134 m^3/sec, 0.0015 m^3/sec, 0.0017 m^3/sec, 0.002 m^3/sec, 0.0022 m^3/sec, 0.0027 m^3/sec, 0.0034 m^3 /sec, and 0.0047 m^3/sec.

2. Dependent Variable

Dependent variables are those variables whose magnitude is influenced by the independent variable. The dependent variables in this study include shaft rotation, turbine output power, and efficiency.

3. Control variable

These are simply constant variables. The control variables used in this study are:

1. The three turbine angle variations, namely 25°, 30°, and 35°.
2. The test time (3 minutes).

2.6 Test flow chart

The test flow is presented in Fig 9.

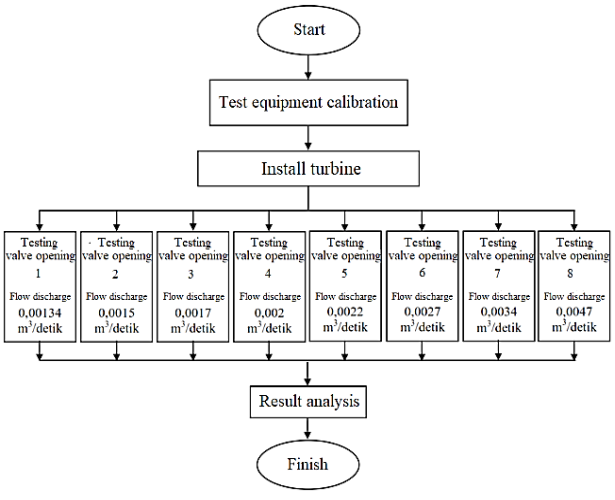

Fig 9. Test Flow Chart

3 Results and Discussion

3.1. Main Dimensions of Turbine Blades

The values required to calculate the runner blade's diameter are listed in section 2. Using these values, the main dimensions of the blades were obtained. These dimensions, as well as the velocities and angles of the occurring triangles, are shown in Tables 1 and 2, respectively.

Table 1. Main Dimensions of Turbine Blades

Parameter	Symbol	Value	Unit
Blade outside diameter	D_e	0,15	[m]
Hub diameter	D_i	0,03	[m]
Blade cross-sectional area	A	0,022	[m]
Blade center diameter	D_c	0,0165	[m]
Total blade width	L	0,135	[m]
Distance between blades	L_1	0,129	[m]

Table 2. Velocity and Angle of the Resulting Velocity Triangle

	$6=\boldsymbol{D_e}$	5	4	3	2	$1=\boldsymbol{D_i}$	
d	0,15	0,126	0,102	0,078	0,054	0,03	[m]
u	8,2	6,29	5,6	4,28	2,97	1,65	[m/s]
c_{u1}	2,95	3,5	4,32	5,65	6,16	7,34	[m/s]
c_{u2}	3,13	3,71	4,58	5,99	6,66	7,79	[m/s]
w_{u1}	-5,25	-3,42	-1,28	1,37	2,71	4,24	[m/s]
w_{u2}	-5,07	-3,21	-1.02	1,71	2,99	4,46	[m/s]
$w_{u\infty}$	-5,16	-3,31	-1,15	-1,54	3,24	4,29	[m/s]
w_m	0,04	0,04	0,04	0,04	0,04	0,04	[m/s]
w_1	5,25	5,34	1,28	1,37	0,19	-1,43	[m/s]
w_2	5,08	3,21	1,02	1,71	0,55	-1,89	[m/s]
w_∞	5,16	3,31	1,15	1,54	0,32	-1,57	[m/s]
β_∞	180	179	178	1	0	0	[°]
$(180-\beta_\infty)$	0	1	2	179	180	180	[°]

3.2. Blade Characteristics

The lift coefficient for each radius was determined using Equation (17). After which the ratio *l/t* was determined using equation (18) with an assumed slip angle value of 3°. The lift coefficient ratio $\zeta a/\zeta A$ could be seen from the reciprocal values in Fig 6 section 2. Using this ratio, the lift ζA and drag coefficient of different profiles were obtained from Fig 7 in section 2, while the slip angle was determined using Equation (19). The main design characteristics of the turbine blades were also obtained and the results are shown in Table 3.

Table 3 Blade Characteristics

Parameter	Symbol	Value	Unit
Lift coefficient	ζa	1,38	[°]
l/t ratio	1/t	-0,084	[-]
t/l ratio	t/l	11,90	[-]
Lifting force coefficient ratio	ζ_a/ζ_A	2,22	[-]
Coefficient of drag	ζ_w	0,0062	[-]
Angle of attack	δ	-5,18	[°]
Distortion angle	(180-β_∞-δ)	9,18	[°]

3.3. Manufacturing Results

Axial flow propeller turbine blades are generally manufactured using casting technology. The cost of producing these blades is high, which significantly led to its high market price. However, it will be cheaper when mass produced. These turbines are typically designed as energy converters in hydroelectric power plants and used for flow in pipes or irrigation flow in rural areas. Accordingly, the manufacture of turbine blades should be done

using available local resources and technologies. The turbine blades constructed in this study are shown in Fig 10

Fig 10. Turbine Runner Blade

Shows Fig 11 is a prototype design of an axial flow pico-propeller turbine with a size of 150 mm and intended to operate at an effective height of 3.5 m with a design flow of 0.0024 m^3/s.

Fig 11. Pico-Propeller Turbine Assembly

3.4 Turbine installation results

The results of installing the turbine at the sewer line test site at PDAM Tirta Meulaboh are shown in Fig 12.

Fig 12. Results of installing a pico-propeller turbine on the PDAM's sewer pipe

3.5. Performance Test Results

The performance test was conducted by first measuring the water flow with a propeller device current meter. The results revealed a temporary flow rate of 0.00242 m^3/s. The amount of shaft rotation obtained as a function of changes in angle and flow discharge is shown in Fig 13.

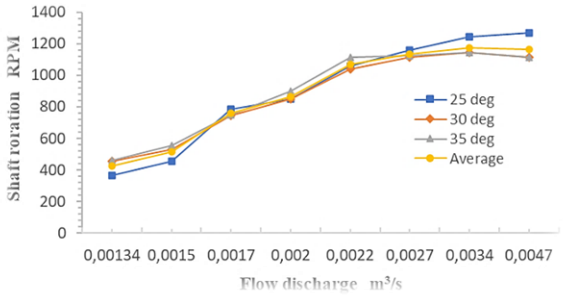

Fig 13. Graph of the Effect of Turbine Blade Angle on Shaft Rotation

Fig 13 shows the relationship between the flow rate, blade angle and shaft rotation. The result showed that the blade's slope had a different maximum performance limit and does not depend on the flow rate of the sewer line. Furthermore, the highest rotation speed (1267 rpm) was obtained at a flow rate of 0.0047 m^3/s with the 25° angled blade, and the lowest speed (365.5 rpm) was obtained at a flow rate of 0.00134 m^3/s with a 30^0 angled blade. Clearly, the turbine's rotation is influenced by its blade angle. It was observed from previous field tests that blades with an angle of 30° or 35° easily rotates during start-up even at low flow rates (0.00134 m^3/s) while the 25° angled blade's rotation is solely dependent on the flow rate. The relationship between the blade angle, flow rate, and torque is shown in Fig 14.

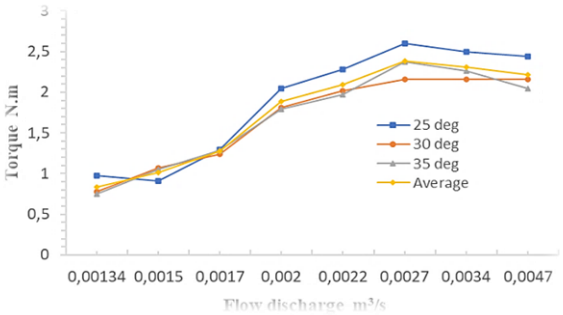

Fig 14. Graph Showing the Relationship of Blade Angle and Flow Discharge versus Torque

Fig 14 shows the effects of turbine blade angle and flow rate on torque power. The results obtained from testing the Pico-propeller turbine prototype showed that the average torque value increased by 0.25 Nm when the flow rate increased. However, when the rotational speed increased to 1176.3 rpm, the torque value decreased by 0.16 Nm. Furthermore, the lowest torque value (0.75 Nm) was obtained with the 35^0 angled blade at a minimum flow rate of 0.00134 m^3/s, and the maximum value (2.60 Nm) was obtained with the blade having an angle of 25° at a 0.0027 m^3/s flow rate. Also, at a constant flow rate, the torque value of both the 30°, and 35° angled blades were observed. The values obtained were 2.16 Nm and 2.38 Nm respectively. Next, the turbine power was analyzed based on the flow rate (Fig 15).

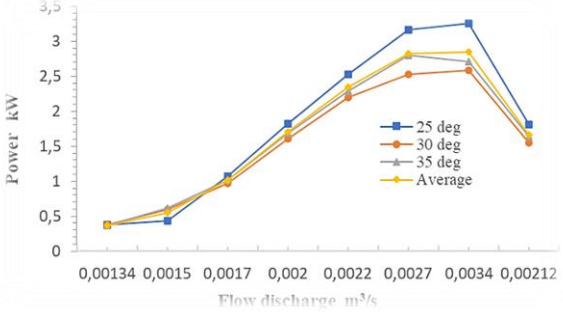

Fig 15. A Graphical Representation of the Effect of Blade Angle and Flow Discharge on Turbine Power

Fig 15 shows the relationship between the flow rate, turbine power, and blade angle variations of 25°, 30°, and 35°. It was observed that the turbine power increased when there was an increase in the flow rate and it decreased when the flow rate increased further to 0.0034 m^3/s. At this rate, the turbine blade rotation was at its maximum. Furthermore, the results shows that the 25^0 angled blades tend to increase power by an average of 0.48 kW at flow rates ranging from 0.00134 m^3/s to 0.0047 m^3/s, and an average rotation speed of 898 rpm. However, the power increased by an average of 0.37 kW at flow rates ranging from 0.0134 m^3/s to 0.0034 m^3/s, and an average rotation speed of 840 rpm for the 30^0 angled blades. The power increased by an average of 0.39 kW for blades with an angle of 35°, at flow rates ranging from 0.00134 m^3/s to 0.0042 m^3/s, and a rotation speed of 863 rpm. The effect of flow rate on the turbine's efficiency is shown in Fig 16.

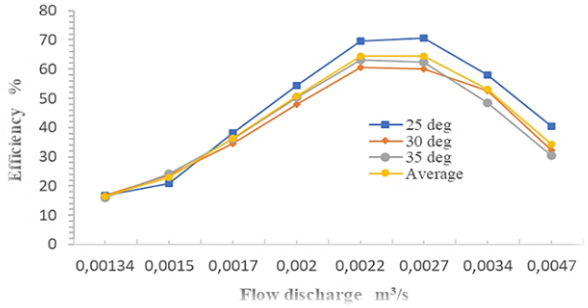

Fig 16. Graph of the Effect of Flow on Efficiency

Fig 16 shows a prototype Pico-propeller turbine with various blade angles as a whole, which can operate optimally at a flow rate of 0.0034 m^3/s. However, the maximum efficiency average was obtained at a flow rate of 0.027 m^3/s, and from the three-blade runner model, it was observed that the 25° angled blade had better efficiency compared to the 30° and 35°.

These results were in line with the design results of the computational scale turbine runner blade model, and the outlined blade shape effects of previous research [20, 22]. The effect of turbine runner blade angle and torque power on efficiency is shown in Fig 17.

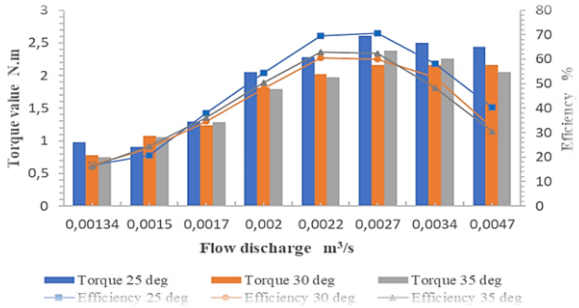

Fig 17. Graph of the Effect of Turbine Blade Angle and Torque Power on Efficiency

Fig 17 shows that the increase in blade's angle proportionally increases efficiency, and decreases torque coefficient. The increase in average efficiency is based on torque power and a 22.29% increase in flow rate. These results are also in line with previous research, which showed that blade number and angle affect turbine performance [23, 24]. Figure 15 also show that the turbine runner blades with an angle of 25° produced higher angular velocity and efficiency compared to those with 30° and 35°. Furthermore, the obtained average efficiency values of the 25°, 30°, and the 35° angled blades were 46.07%, 41.025%, and 41.40%, respectively. The highest efficiency (70.67%) and torque coefficient (26%) was obtained with the 25% angled blades at a 0.0027 m^3/s flow rate. While the lowest efficiency (16.1%) and torque coefficient (0.75%) was obtained with the 35% angled blades. These results also confirm the previous research findings by [25].

4 Conclusion

The turbine runner blade's rotation speed is not only determined by the head and flow discharge but also by the influence of its geometric shape and angle of inclination. These energies cause the thrust force of water entering the pipe (inlet) to pound the surface of the turbine blades before exiting. Therefore, head, flow rate, and turbine-specific speed are three critical variables that must be considered when planning blade dimensions.

Furthermore, the different angled blades design was built based on the relationship between the absolute speed (v), rotational speed (c), and relative speed (u). This is an essential factor because it provides an understanding of the vectors acting on the turbine blades. Therefore, the shape of the turbine blades can be formed at each change point based on the speed of the moving water, and its efficiency can be calculated either by simulation or by experiment.

In addition, the slope angle parameter of the runner blades shows that the turbine performance is affected by the axial force received by each blade, the interactions between the blade's angle, and the flow rate. The blade angle has a more dominant influence on the turbine design flow characteristics. However, the blade's performance efficiency consistently showed a non-linear characteristic trend that increased to the peak of the optimal value, after which it decreased when the slope of the blade's angle was increased. Finally, from the three turbine blade models designed, it was found that the 25° angled blade had better efficiency than 30° and 35° at a flow rate of 0.0027 m^3/s.

Acknowledgment

The authors are grateful to the Regional Water Company (PDAM) Tirta Meulaboh for providing technical support during this study.

References

[1] S. Phitaksurachai, R. Pan-Aram, N. Sritrakul, and Y. Tiaple, "Performance Testing of Low Head Small Hydro Power Development in Thailand," *Energy Procedia*, vol. 138, pp. 1140–1146, 2017.

[2] Republik Indonesia, Government Regulation of the Republic of Indonesia No. 22 concerning the General Plan of National Energy. 2017.

[3] A. T. A. 2006 Purwanto. W. W., Nugroho. Y. S., Rinaldy. D., Harsono. S., Wahid. A., Supramono. D., Herminna. D., *Indonesia Energy Outlook and Statistics 2006*. Pengkajian Energi Universitas Indonesia Gedung Engineering Center Lantai 3 Fakultas Teknik Universitas Indonesia Depok, 2006.

[4] A. Tasri and A. Susilawati, "Selection among renewable energy alternatives based on a fuzzy analytic hierarchy process in Indonesia," *Sustain. Energy Technol. Assessments*, vol. 7, pp. 34–44, 2014.

[5] A. Date and A. Akbarzadeh, "Design and cost analysis of low head simple reaction hydro turbine for remote area power supply," *Renew. Energy*, vol. 34, no. 2, pp. 409–415, 2009.

[6] A. A. Ghadimi, F. Razavi, and B. Mohammadian, "Determining optimum location and capacity for micro hydropower plants in Lorestan province in Iran," *Renew. Sustain. Energy Rev.*, vol. 15, no. 8, pp. 4125–4131, 2011.

[7] J. A. Laghari, H. Mokhlis, A. H. A. Bakar, and H.

Mohammad, “A comprehensive overview of new designs in the hydraulic, electrical equipments and controllers of mini hydro power plants making it cost effective technology,” *Renew. Sustain. Energy Rev.*, vol. 20, pp. 279–293, 2013.
[8] C. P. Jawahar and P. A. Michael, “A review on turbines for micro hydro power plant,” *Renewable and Sustainable Energy Reviews*, vol. 72. Elsevier Ltd, pp. 882–887, 2017.
[9] H. Zainuddin, A. Khamis, M. S. Yahaya, M. F. M. Basar, J. M. Lazi, and Z. Ibrahim, “Investigation on the performance of pico-hydro generation system using consuming water distributed to houses,” *Proc. 1st Int. Conf. Dev. Renew. Energy Technol. ICDRET 2009*, pp. 210–213, 2009.
[10] H. M. Ramos, M. Simão, and K. N. Kenov, “Low-Head Energy Conversion: A Conceptual Design and Laboratory Investigation of a Microtubular Hydro Propeller,” *ISRN Mech. Eng.*, vol. 2012, pp. 1–10, 2012.
[11] C. Trivedi, M. J. Cervantes, and O. G. Dahlhaug, “Numerical Techniques Applied to Hydraulic Turbines: A Perspective Review,” *Appl. Mech. Rev.*, vol. 68, no. 1, pp. 1–18, 2016.
[12] L. L. Oo, S. Y. Win, and K. Z. Lin, “Design of Blade for 5kW Propeller Turbine,” *Int. J. Sci. Eng. Appl.*, vol. 7, no. 10, pp. 336–340, 2018.
[13] Y. Nishi, Y. Kobayashi, T. Inagaki, and N. Kikuchi, “The Design Method of Axial Flow Runners Focusing on Axial Flow Velocity Uniformization and Its Application to an Ultra-Small Axial Flow Hydraulic Turbine,” *Int. J. Rotating Mach.*, pp. 1–13, 2016.
[14] R. S. Shukla and C. Parashar, “Design of Propeller Turbine for Micro Hydro Power Station Using CFD,” vol. 1, no. 7, pp. 37–41, 2017.
[15] S. Byeon and Y. Kim, “Influence of Blade Number on the Flow Characteristics in the Vertical Axis Influence of Blade Number on the Flow Characteristics in the Vertical Axis Propeller Hydro Turbine,” vol. 6, no. 3, pp. 144–151, 2013.
[16] European Small Hydropower Association - ESHA, “Electromechanical Equipment,” *Guid. how to Dev. a small hydropower plant*, vol. 6, no. 3, pp. 154–196, 2004.
[17] S. L. Dixon, “Fluid Mechanics and Thermodynamics of Turbomachinery,” no. 14, Elsevier Inc., 2014, pp. 361–418.
[18] S. L. Dixon, *Fluid Mechanics And Thermodynamics of Turbomachinery*, Sixth Edit. Elsevier Inc., 2010.
[19] Rama S. R. Gorla, *Turbomachinery Design and Theory*. Marcel Dekker.Inc, 2003.
[20] P. Pribadyo, H. Hadiyanto, and J. Jamari, “Computational fluid dynamic (CFD) analysis of propeller turbine runner blades using various blade angles,” *Int. Energy J.*, vol. 21, no. 3, pp. 385–400, 2021.
[21] R. Simpson and A. Williams, “Design of propeller turbines for pico hydro,” pp. 1–15, 2011.
[22] V. L. Vu, Z. Chen, and Y.-D. Choi, “Design and Performance of a Pico Propeller Hydro Turbine Model,” *KSFM J. Fluid Mach.*, vol. 21, no. 3, pp. 44–51, 2018.
[23] P. Singh and F. Nestmann, “Influence of the Blade Hub Geometry on the Performance of Low-Head Axial Flow Turbines,” no. September, pp. 109–118, 2012.
[24] S. S. Byeon, J. H. Boo, J. Y. Park, S. S. Kim, and Y. J. Kim, “Numerical study on the flow characteristics of low head small hydraulic turbine,” *Adv. Mater. Res.*, vol. 732–733, pp. 436–442, 2013.
[25] S. Kim, Y. Choi, Y. Cho, J. Choi, and J. Kim, “Effect of Blade Thickness on the Hydraulic Performance of a Francis Hydro Turbine Model,” *Renew. Energy*, vol. 6, no. 3, pp. 144–151, 2018.